

Hadronic Spectral Functions in Lattice QCD

Y. Nakahara⁽¹⁾, M. Asakawa⁽¹⁾, and T. Hatsuda⁽²⁾

⁽¹⁾ *Department of Physics, Nagoya University, Nagoya 464 - 8602, Japan*

⁽²⁾ *Physics Department, Kyoto University, Kyoto 606-8502, Japan*

(May 19, 2019)

QCD spectral functions of hadrons in the pseudo-scalar and vector channels are extracted from lattice Monte Carlo data of the imaginary time Green's functions. The maximum entropy method works well for this purpose, and the resonance and continuum structures in the spectra are obtained in addition to the ground state peaks.

12.38.Gc, 12.38.Aw

Among various dynamical quantities in quantum chromodynamics (QCD), the spectral functions (SPFs) of hadrons play a special role in physical observables (See e.g. [1,2]). A well-known example is the cross section of the e^+e^- annihilation into hadrons, which can be expressed by SPF in the vector channel. SPF at finite temperature (T) and/or baryon density is also a key concept to understand the modification of hadrons in hot and/or dense medium [3]. The enhancement in low mass dileptons observed in relativistic heavy ion collisions at CERN SPS [4] is a typical example which may indicate spectral shift in the medium [5].

However, the Monte Carlo simulations of QCD on the lattice, which have been successful in measuring static observables [6], have difficulties in accessing the dynamical quantities in the Minkowski space such as SPFs and the real time correlation functions. This is because measurements on the lattice can only be carried out for discrete points in imaginary time. The analytic continuation from the imaginary time to the real time using the finite number of lattice data with noise is highly non-trivial and is even classified as an ill-posed problem.

In this Letter, we make a first serious attempt to extract SPFs of hadrons from lattice QCD data without making a priori assumptions on the spectral shape. For this purpose, we use the maximum entropy method (MEM), which has been successfully applied for similar problems in quantum Monte Carlo simulations in condensed matter physics, image reconstruction in crystallography and astrophysics, and so forth [7,8]. Due to the limitation of space, we present only the results for the pseudo-scalar (PS) and vector (V) channels at $T = 0$. The results for other channels will be given in the forthcoming paper [9].

The Euclidean correlation function $D(\tau)$ of a Heisenberg operator $\mathcal{O}(\tau, \vec{x})$ and its spectral decomposition read

$$D(\tau \geq 0) = \int d^3x \langle \mathcal{O}^\dagger(\tau, \vec{x}) \mathcal{O}(0, \vec{0}) \rangle \quad (1)$$

$$= \int_0^\infty K(\tau, \omega) A(\omega) d\omega. \quad (2)$$

The spatial integration in eq.(1) picks up only the states with zero three-momentum. ω is a real frequency and $A(\omega)$ is SPF (or sometimes called the *image* in this Letter), which is positive semi-definite by definition. The kernel $K(\tau, \omega)$ is proportional to the Fourier transform of a free boson propagator with mass ω : At $T = 0$, $K(\tau, \omega) = \exp(-\tau\omega)$.

Monte Carlo simulation provides $D(\tau_i)$ for the discrete set of points $0 \leq \tau_i/a \leq N_\tau$, where N_τ is the temporal lattice size and a is the lattice spacing. In the actual analysis, we use data points for $\tau_{min} \leq \tau_i \leq \tau_{max}$. From this data set with noise, we need to reconstruct the continuous function $A(\omega)$ on the right hand side of (2). This is a typical ill-posed problem, where the number of data is much smaller than the number of degrees of freedom to be reconstructed. MEM is a method to circumvent this difficulty by making a statistical inference of the most probable *image* as well as its reliability [7].

The theoretical basis of MEM is the Bayes' theorem in probability theory: $P[X|Y] = P[Y|X]P[X]/P[Y]$, where $P[X|Y]$ is the conditional probability of X given Y . Let D stand for Monte Carlo data with errors for a specific channel on the lattice and H summarize all the definitions and prior knowledge such as $A(\omega) \geq 0$. The most probable image $A(\omega)$ for given lattice data is obtained by maximizing the conditional probability $P[A|DH]$, which, by the Bayes' theorem, is rewritten as

$$P[A|DH] \propto P[D|AH]P[A|H], \quad (3)$$

where $P[D|AH]$ ($P[A|H]$) is called the likelihood function (the prior probability).

For the likelihood function, the central limiting theorem leads to $P[D|AH] = Z_L^{-1} \exp(-L)$ with

$$L = \frac{1}{2} \sum_{i,j} (D(\tau_i) - D^A(\tau_i)) C_{ij}^{-1} (D(\tau_j) - D^A(\tau_j)), \quad (4)$$

where i and j run from τ_{min}/a through τ_{max}/a . Z_L is a normalization factor given by $Z_L = (2\pi)^{N/2} \sqrt{\det C}$ with $N = \tau_{max}/a - \tau_{min}/a + 1$. $D(\tau_i)$ is the lattice data averaged over gauge configurations and $D^A(\tau_i)$ is the correlation function defined by the right hand side of (2). C is an $N \times N$ covariance matrix defined by $C_{ij} = [N_{conf}(N_{conf} - 1)]^{-1} \sum_{m=1}^{N_{conf}} \Delta_i^m \Delta_j^m$. Here N_{conf} is the total number of gauge configurations and $\Delta_i^m \equiv$

$D^m(\tau_i) - D(\tau_i)$ with $D^m(\tau_i)$ being the data for the m -th gauge configuration. The lattice data have generally strong correlations among different τ 's, and it is essential to take into account the off-diagonal components of C .

It can be generally shown on an axiomatic basis [10] that, for positive distributions such as SPF, the prior probability can be written with parameters α and m as $P[A|H\alpha m] = Z_S^{-1} \exp(\alpha S)$. Here S is the Shannon-Jaynes entropy,

$$S = \int_0^\infty \left[A(\omega) - m(\omega) - A(\omega) \log \left(\frac{A(\omega)}{m(\omega)} \right) \right] d\omega. \quad (5)$$

Z_S is a normalization factor: $Z_S \equiv \int e^{\alpha S} \mathcal{D}A$. α is a real and positive parameter and $m(\omega)$ is a real function called the default model.

In this Letter, we adopt a state-of-art MEM [7], where the output image A_{out} is given by a weighted average over A and α :

$$\begin{aligned} A_{out}(\omega) &= \int A(\omega) P[A|DH\alpha m] P[\alpha|DHm] \mathcal{D}A d\alpha \\ &\simeq \int A_\alpha(\omega) P[\alpha|DHm] d\alpha. \end{aligned} \quad (6)$$

Here $A_\alpha(\omega)$ is obtained by maximizing $Q \equiv \alpha S - L$ for a given α with an assumption that $P[A|DH\alpha m]$ is sharply peaked around $A_\alpha(\omega)$. α dictates the relative weight of the entropy S (which tends to fit A to the default model m) and the likelihood function L (which tends to fit A to the lattice data). Note, however, that α appears only in the intermediate step and is integrated out in the final result. We found that the weight factor $P[\alpha|DHm]$, which is calculable using Q [7], is highly peaked around its maximum $\alpha = \hat{\alpha}$ in our lattice data. One can also study the stability of the $A_{out}(\omega)$ against a reasonable variation of $m(\omega)$.

The non-trivial part of the MEM analysis is to find the global maximum of Q in the functional space of $A(\omega)$, which has typically 750 degrees of freedom in our case. We have utilized the singular value decomposition method to define the search direction in this functional space. The method works successfully to find the global maximum within reasonable iteration steps. The technical details will be given in [9].

To check the feasibility of the MEM procedure and to see the dependence of the MEM image on the quality of the data, we made the following test using mock data. (i) We start with an input image $A_{in}(\omega) \equiv \omega^2 \rho_{in}(\omega)$ in the ρ -meson channel which simulates the experimental e^+e^- cross section. Then we calculate $D(\tau)$ from $A_{in}(\omega)$ using eq.(2). (ii) By taking $D(\tau_i)$ at N discrete points and adding a Gaussian noise, we create a mock data $D_{mock}(\tau_i)$. The variance of the noise $\sigma(\tau_i)$ is given by $\sigma(\tau_i) = b \times D(\tau_i) \times \tau_i/a$ with a parameter b , which controls the noise level [11]. (iii) We construct the output image $A_{out}(\omega) \equiv \omega^2 \rho_{out}(\omega)$ using MEM with

$D_{mock}(\tau_{min} \leq \tau_i \leq \tau_{max})$ and compare the result with $A_{in}(\omega)$. In this test, we have assumed that C is diagonal for simplicity.

In Fig.1, we show $\rho_{in}(\omega)$, and $\rho_{out}(\omega)$ for two sets of parameters, (I) and (II). As for m , we choose a form $m(\omega) = m_0 \omega^2$ with $m_0 = 0.027$, which is motivated by the asymptotic behavior of A in perturbative QCD, $A(\omega \gg 1\text{GeV}) = (1/4\pi^2)(1 + \alpha_s/\pi)\omega^2$. The final result is, however, insensitive to the variation of m_0 even by factor 5 or 1/5. The calculation of $A_{out}(\omega)$ has been done by discretizing the ω -space with an equal separation of 10 MeV between adjacent points. This number is chosen for the reason we shall discuss below. The comparison of the dashed line (set (I)) and the dash-dotted line (set (II)) shows that increasing τ_{max} and reducing the noise level b lead to better SPFs closer to the input SPF.

We have then applied MEM to actual lattice data. For this purpose, quenched lattice QCD simulations have been done with the plaquette gluon action and the Wilson quark action by the open MILC code with minor modifications [12]. The lattice size is $20^3 \times 24$ with $\beta = 6.0$, which corresponds to $a = 0.0847$ fm ($a^{-1} = 2.33$ GeV), $\kappa_c = 0.1571$ [13], and the spatial size of the lattice $L_s a = 1.69$ fm. Gauge configurations are generated by the heat-bath and over-relaxation algorithms with a ratio 1 : 4. Each configuration is separated by 1000 sweeps. Hopping parameters are chosen to be $\kappa = 0.153, 0.1545$, and 0.1557 with $N_{conf} = 161$ for each κ . For the quark propagator, the Dirichlet (periodic) boundary condition is employed for the temporal (spatial) direction. To calculate the two-point correlation functions, we adopt a point-source at $\vec{x} = 0$ and a point-sink averaged over the spatial lattice-points to extract physical states with vanishing three-momentum. For the PS and V channels, the operators $\bar{d}\gamma_5 u$ and $\bar{d}\gamma_\mu u$ ($\mu = 1, 2, 3$) are chosen, respectively. We use data at $1 \leq \tau_i/a \leq 12$ to remove the noise at the Dirichlet boundary. To avoid the known pathological behavior of the eigenvalues of C [7], we take $N_{conf} \gg N$.

We define SPFs for the PS and V channels, respectively, as

$$A(\omega) = \omega^2 \rho_{PS}(\omega) \quad \text{and} \quad A(\omega) = \omega^2 \rho_V(\omega), \quad (7)$$

so that $\rho_{PS,V}(\omega \rightarrow \text{large})$ approaches a finite constant as predicted by perturbative QCD. For the MEM analysis, we need to discretize ω , and need to choose $\Delta\omega$ (the mesh size) and ω_{max} (the upper limit for the ω integration) in eq.(2). Since $\Delta\omega$ should be much smaller than $1/\tau_{max}$ to suppress the discretization error, we take $\Delta\omega = 10$ MeV. ω_{max} should be comparable to the maximum available momentum on the lattice: $\omega_{max} \sim \pi/a \sim 7.3$ GeV. We have checked that larger values of ω_{max} do not change the result of $A(\omega)$ substantially, while smaller values of ω_{max} distort the high energy end of the spectrum. The dimension of the image to be reconstructed

is $N_\omega \equiv \omega_{max}/\Delta\omega \simeq 750$, which is in fact much larger than the maximum number of Monte Carlo data $N = 25$. This makes the standard likelihood analysis and its variants inapplicable [14] unless strong assumptions on the spectral shape are made, while MEM does not suffer from such difficulties. In the MEM analysis of the lattice data, we have used the kernel $K = \exp(-\tau\omega)$. One may alternatively use the kernel defined on the lattice. The detailed comparison of these two cases will be given in [9].

In Fig.2 (a) and (b), we show the reconstructed images for each κ . In these figures, we have used $m = m_0\omega^2$ with $m_0 = 2.0(0.86)$ for PS (V) channel motivated by the perturbative estimate of m_0 (see eq.(8) and the text below). We have checked that the result is not sensitive, within the statistical significance of the image, to the variation of m_0 by factor 5 or 1/5. The obtained images have a common structure: the low-energy peaks corresponding to π and ρ , and the broad structure in the high-energy region. From the position of the pion peaks in Fig.2(a), we extract $\kappa_c = 0.1570(3)$, which is consistent with 0.1571 [13] determined from the asymptotic behavior of $D(\tau)$. The mass of the ρ -meson in the chiral limit extracted from the peaks in Fig.2(b) reads $m_\rho a = 0.348(15)$. This is also consistent with $m_\rho a = 0.331(22)$ [13] determined by the asymptotic behavior. Although our maximum value of the fitting range $\tau_{max}/a = 12$ marginally covers the asymptotic limit in τ , we can extract reasonable masses for π and ρ . The width of π and ρ in Fig.2 is an artifact due to the statistical errors of the lattice data. In fact, in the quenched approximation, there is no room for the ρ -meson to decay into two pions.

As for the second peaks in the PS and V channels, the error analysis discussed in Fig.3 shows that their spectral ‘‘shape’’ does not have much statistical significance, although the existence of the non-vanishing spectral strength is significant. Under this reservation, we fit the position of the second peaks and made linear extrapolation to the chiral limit with the results, $m^{2nd} = 1.524(3)(1.981(13))$ MeV for the PS (V) channel with $a^{-1} = 2.33$ GeV. They are 20-40 % heavier than the observed resonances, $\pi(1300)$ and $\rho(1450)$.

One should remark here that, in the standard two-mass fit of $D(\tau)$ [13], the mass of the second resonance is highly sensitive to the lower limit of the fitting range τ_{min} . This is because the contamination from the short distance contributions from $\tau < \tau_{min}$ is not under control in such an approach. On the other hand, MEM does not suffer from this difficulty and can utilize the full information down to $\tau_{min}/a = 1$. Therefore, MEM opens a possibility of systematic study of higher resonances with lattice QCD data.

As for the third bumps in Fig.2, the spectral ‘‘shape’’ is statistically not significant as is discussed in Fig.3, and they should rather be considered a part of the perturbative continuum instead of a single resonance. Fig.2

also shows that SPF decreases substantially above 6 GeV; MEM automatically detects the existence of the momentum cutoff on the lattice $\sim \pi/a$. It is expected that MEM with the data on finer lattices leads to larger ultra-violet cut-offs in the spectra. The height of the asymptotic form of the spectrum at high energy is estimated as

$$\rho_V(\omega \simeq 6\text{GeV}) = \frac{1}{4\pi^2} \left(1 + \frac{\alpha_s}{\pi}\right) \left(\frac{1}{2\kappa Z_V}\right)^2 \simeq 0.86. \quad (8)$$

The first two factors are the $q\bar{q}$ continuum expected from perturbative QCD. The third factor contains the non-perturbative renormalization constant for the lattice composite operator. We adopt $Z_V = 0.57$ determined from the two-point functions at $\beta = 6.0$ [15] together with $\alpha_s = 0.21$ and $\kappa = 0.1557$. Our estimate in eq.(8) is consistent with the high energy part of the spectrum in Fig.2(b) after averaging over ω . We made a similar estimate for the PS channel using $Z_{PS} = 0.49$ [16] and obtained $\rho_{PS}(\omega \simeq 6\text{GeV}) \simeq 2.0$. This is also consistent with Fig. 2(a). We note here that an independent analysis of the imaginary time correlation functions [2] also shows that the lattice data at short distance is dominated by the perturbative continuum.

Within the MEM analysis, one can study the statistical significance of the reconstructed image by the following procedure [7]. Assuming that $P[A|DH\alpha m]$ has a Gaussian distribution around the most probable image \hat{A} , we estimate the error by the covariance of the image, $\langle\langle(\delta_A\delta_A Q)^{-1}\rangle\rangle_{A=\hat{A}}$, where δ_A is a functional derivative and $\langle\cdot\rangle$ is an average over a given energy interval. The final error for A_{out} is obtained by averaging the covariance over α with a weight factor $P[\alpha|DHm]$. Shown in Fig.3 is the MEM image in the V channel for $\kappa = 0.1557$ with errors obtained in the above procedure. The height of each horizontal bar is $\langle\rho_{out}(\omega)\rangle$ in each ω interval. The vertical bar indicates the error of $\langle\rho_{out}(\omega)\rangle$. The small error for the lowest peak in Fig.3 supports our identification of the peak with ρ . Although the existence of the non-vanishing spectral strength of the 2nd peak and 3rd bump is statistically significant, their spectral ‘‘shape’’ is either marginal or insignificant. Lattice data with better quality are called for to obtain better SPFs.

In summary, we have made a first serious attempt to reconstruct SPFs of hadrons from lattice QCD data. We have used MEM, which allows us to study SPFs without making a priori assumption on the spectral shape. The method works well for the mock data. Even for the lattice data, the method produces resonance and continuum-like structures in addition to the ground state peaks. The statistical significance of the image has been also analyzed. Better data with finer and larger lattice will produce better images with smaller errors, and our study should be considered a first attempt towards this goal. We have not made the chiral extrapolation of SPFs in this Letter, since we have found that neither the direct extrapolation

of the MEM image $A_{out}(\omega)$ nor the extrapolation of $D(\tau)$ and C works in a straightforward manner. We leave this as an open problem. From the physics point of view, the spectral change at finite temperature is by far the important problem. This is currently under investigation.

We appreciate MILC collaboration for their open codes for lattice QCD simulations, which has enabled this research. Our simulation was carried out on a Hitachi SR2201 parallel computer at Japan Atomic Energy Research Institute. M. A. (T. H.) was partly supported by Grant-in-Aid for Scientific Research No. 10740112 (No. 10874042) of the Japanese Ministry of Education, Science, and Culture. T. H. was also supported by Sumitomo Foundation (Grant No. 970248).

-
- [1] E. V. Shuryak, *Rev. Mod. Phys.* **65**,1 (1993).
 - [2] M. -C. Chu, J. M. Grandy, S. Huang, and J. W. Negele, *Phys. Rev. D* **48**, 3340 (1993).
 - [3] For early references on SPFs in the medium, see e.g. C. Gale and J. Kapusta, *Nucl. Phys.* **B357**, 65 (1991); M. Asakawa and C. M. Ko, *Phys. Rev. C* **48**, R526 (1993); T. Hatsuda, Y. Koike, and S. H. Lee, *Nucl. Phys.* **B394**, 221 (1993). See also a recent review, S. H. Lee, *Nucl. Phys.* **A638**, 183c (1998).
 - [4] G. Agakichiev et al., CERES Collaboration, *Phys. Rev. Lett.* **75**, 1272 (1995); *Nucl. Phys.* **A638**, 159 (1998).
 - [5] G. Q. Li, C. M. Ko, and G. E. Brown, *Phys. Rev. Lett.* **75**, 4007 (1995).
 - [6] Lattice 98 Proceedings, to be published in *Nucl. Phys. Proc. Suppl.* (1999); hep-lat/9811023.
 - [7] See the review, M. Jarrell and J. E. Gubernatis, *Phys. Rep.* **269**, 133 (1996).
 - [8] R. N. Silver et al., *Phys. Rev. Lett.* **65**, 496 (1990); W. von der Linden, R. Preuss, and W. Hanke, *J. Phys.* **8**, 3881 (1996); N. Wu, *The Maximum Entropy Method*, (Springer-Verlag, Berlin, 1997).
 - [9] Y. Nakahara, M. Asakawa, and T. Hatsuda, in preparation.
 - [10] See e.g., J. Skilling, in *Maximum Entropy and Bayesian Methods*, ed. J. Skilling (Kluwer, London, 1989), pp.45-52; S. F. Gull, *ibid.* pp.53-71.
 - [11] This formula is motivated by our actual lattice QCD data.
 - [12] The MILC code ver. 5, <http://cliodhna.cop.uop.edu/~hetrick/milc>.
 - [13] Y. Iwasaki et al., *Phys. Rev. D* **53**, 6443 (1996); T. Bhattacharya et al., *ibid.* 6486.
 - [14] D. B. Leinweber, *Phys. Rev. D* **51**, 6369 (1995); C. Allton and S. Capitani, *Nucl. Phys.* **B526**, 463 (1998); Ph. de Forcrand et al., *Nucl. Phys. B (Proc. Suppl.)* **63A-C**, 460 (1998).
 - [15] L. Maiani and G. Martinelli, *Phys. Lett.* **B178**, 265 (1986).
 - [16] M. Göckeler et al., *Nucl. Phys.* **B544**, 699 (1999).

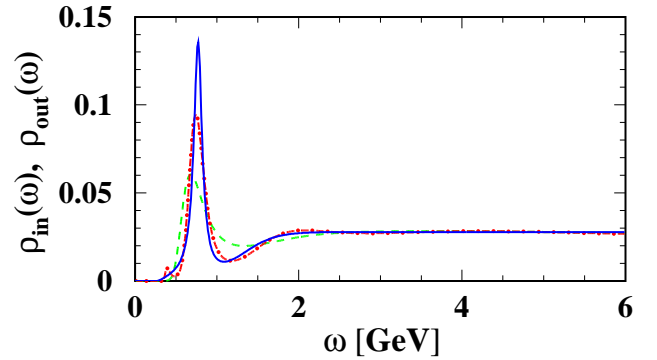


FIG. 1. The solid line is $\rho_{in}(\omega)$. The dashed line and dash-dotted line are $\rho_{out}(\omega)$ obtained with parameter set (I) $a = 0.0847$ fm, $1 \leq \tau/a \leq 12$, $b = 0.001$ and set (II) $a = 0.0847$ fm, $1 \leq \tau/a \leq 36$, $b = 0.0001$, respectively.

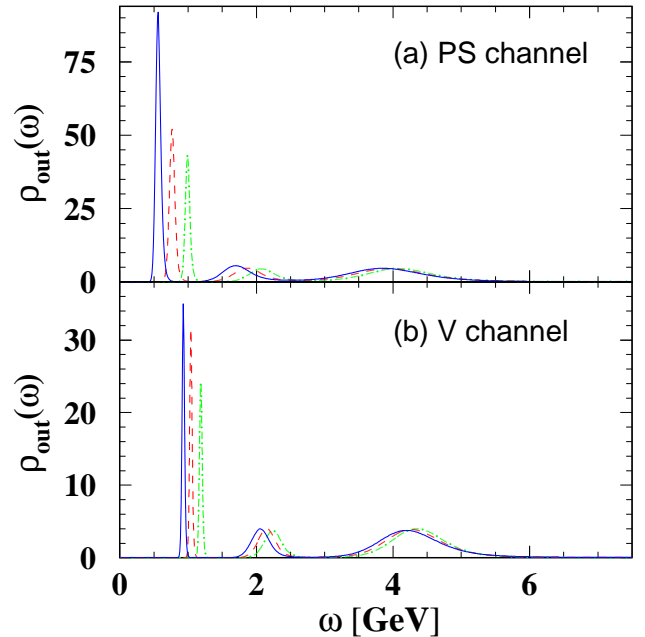


FIG. 2. Reconstructed image $\rho_{out}(\omega)$ for the PS (a) and V (b) channels. The solid, dashed, and dash-dotted lines are for $\kappa = 0.1557$, 0.1545, and 0.153, respectively. For the PS (V) channel, m_0 is taken to be 2.0 (0.86). ω_{max} is 7.5 GeV in this figure and Fig.3.

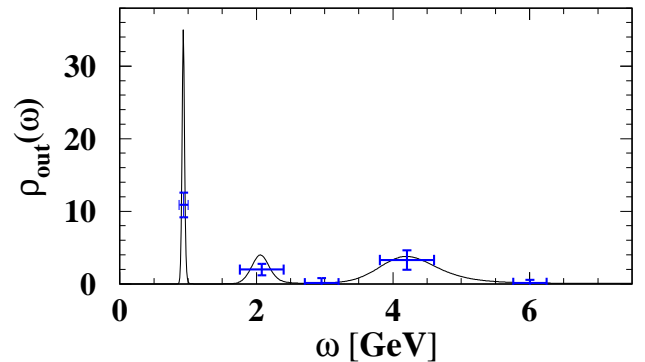


FIG. 3. $\rho_{out}(\omega)$ in the V channel for $\kappa = 0.1557$ with error attached.